

This document is the unedited Author's version of a Submitted Work that was subsequently accepted for publication in ACS Energy Letters, copyright © American Chemical Society after peer review. To access the final edited and published work see <https://doi.org/10.1021/acsenergylett.6b00047>.

Access to this work was provided by the University of Maryland, Baltimore County (UMBC) ScholarWorks@UMBC digital repository on the Maryland Shared Open Access (MD-SOAR) platform.

Please provide feedback

Please support the ScholarWorks@UMBC repository by emailing scholarworks-group@umbc.edu and telling us what having access to this work means to you and why it's important to you. Thank you.

Electron Transfer from Single Semiconductor Nanocrystals to Individual Acceptor Molecules

Haixu Leng,¹ James Loy,¹ Victor Amin,^{2,†} Emily A. Weiss,² and Matthew Pelton^{1,3,}*

¹ Department of Physics, University of Maryland, Baltimore County, 1000 Hilltop Circle,
Baltimore, MD 21250

² Department of Chemistry, Northwestern University, 145 Sheridan Road, Evanston, Illinois
60208

³ Center for Nanoscale Materials, Argonne National Laboratory, 9700 S. Cass Ave., Argonne, IL
60639

AUTHOR INFORMATION

Corresponding Author

* mpelton@umbc.edu

Present Addresses

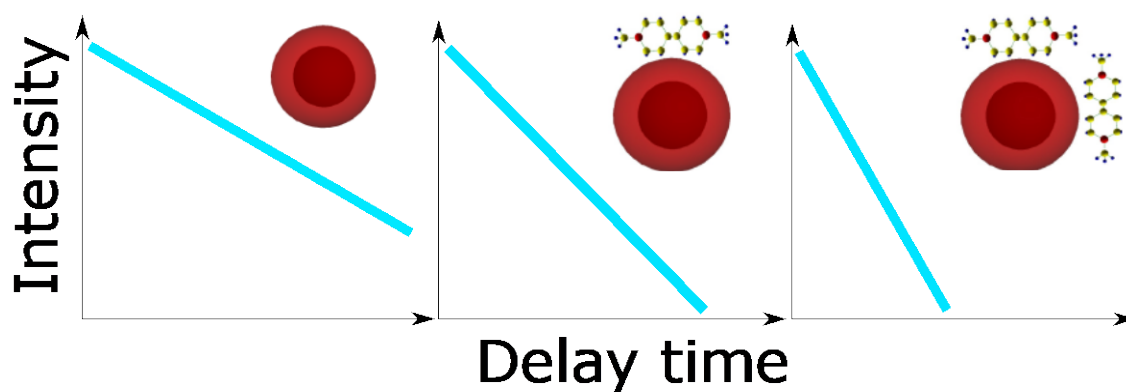
† SendGrid, 1451 Larimer St. #200, Denver, CO 80202

ABSTRACT

This Letter reports the measurement of photoinduced electron-transfer rates from individual CdSe/CdS nanocrystals, or quantum dots (QDs), to methyl viologen acceptor molecules

adsorbed on the QD surfaces, using time-resolved photoluminescence at the single-nanocrystal level. For each QD measured, the electron-transfer rate is constant over time, and the photoluminescence blinking dynamics are independent of the measured transfer rate. The total electron-transfer rate is distributed in discrete, constant increments, corresponding to discrete numbers of adsorbed molecules on each QD. The results thus validate previous assumptions that viologen molecules adsorb independently on QD surfaces and that the total electron-transfer rate from a single QD to multiple molecules on its surface is simply the sum of the transfer rates to the individual molecules. The measurement provides an optical method to count the number of active acceptor molecules bound to a single nanocrystal, and opens up new possibilities for mechanistic studies of charge transfer at the nanoscale.

TOC GRAPHIC



Hybrid structures based on a combination of semiconductor nanocrystals and other organic or inorganic materials have the potential to serve as the basis of next-generation photovoltaic^{1,2} and photocatalytic devices.³ A major reason that the potential of these devices has not yet been realized is the difficulty of efficiently extracting charges from the nanocrystals after photo-excitation. Charge transfer from the nanocrystal to the surrounding material must compete with several other processes, particularly trapping by defect states on the surfaces of the QDs. Understanding how photoinduced charge transfer can be controlled by tuning the structure and chemical makeup of the nanocrystal and the nanocrystal-acceptor interface is a central outstanding problem in this field.^{4,5}

CdSe and CdS quantum dots (QDs) have been used extensively as model systems for studies of photoinduced charge transfer from semiconductor nanocrystals.⁵ Most of these studies have involved photoluminescence or transient-absorption measurements of ensembles of nanocrystals with charge-accepting species adsorbed on their surfaces. These ensemble measurements have enabled comparison of charge-transfer rates with the predictions of Marcus theory,⁶⁻⁸ but data analysis is complicated by heterogeneities within the ensembles of QD-acceptor complexes. This heterogeneity exists not only in the size and shape of the QDs, but also in the number of acceptor molecules adsorbed on the surface of each QD. Quantitative analysis of the ensemble data thus requires fitting to a model with several simplifying assumptions,^{9,10} including independent adsorption of individual molecules on the QD surfaces, and independent, equal, and time-invariant charge-transfer rates to each adsorbed molecule.

An important step towards overcoming the limitations of ensemble heterogeneity was made by measuring photoinduced charge-transfer dynamics from single QDs.¹¹⁻¹⁵ In these measurements, charge transfer from a QD to an acceptor was observed as a decrease in the photoluminescence

lifetime of excitons in the QD. However, these measurements have not yet distinguished QDs according to the number of molecules on their surfaces, and have thus not yet determined the full distribution of transfer rates across the QDs in the ensemble. The distribution has been partially resolved in the case of energy transfer (rather than charge transfer) from single semiconductor nanocrystals to individual adsorbed molecules, through the observation of discrete photobleaching steps.¹⁶ Here, we extend this previous work and report the first measurements of photoinduced electron-transfer rates from single QDs to resolvable numbers of molecules on their surfaces, with the transfer rate increasing in discrete steps as the number of adsorbed molecules increases. These steps are reminiscent of the discrete steps that have been observed in the conductance through molecular junctions;¹⁷ in other words, we provide an optical measurement of electron transfer to individual molecules that complements electrical measurements of electron transport through individual molecules.

The ability to make the optical measurements requires the use of QDs with high photoluminescence quantum yield, so that a large number of photons can be collected from each QD and lifetimes can be accurately determined. A charge-transfer event from a QD to a molecule will quench photoluminescence from the QD; in order to have a measurable photoluminescence signal, the probability that an exciton in the QD is quenched by a charge-transfer event cannot greatly exceed the probability that the exciton recombines and emits a photon. In other words, the charge-transfer rate cannot be much greater than the radiative recombination rate in the QD. At the same time, in order for changes in exciton lifetime due to charge transfer to be resolvable experimentally, they must exceed natural variations in exciton lifetime among QDs in the ensemble. These requirements can be met by CdSe/CdS core/shell QDs: the shell isolates holes from the surface, minimizing hole-trapping events that reduce

quantum yield, and the charge-transfer rate to molecules on the QD surfaces can be precisely controlled by tuning the shell thickness.¹⁸⁻²⁰ Recently developed methods enable the synthesis of high-quality CdSe/CdS core/shell QDs with precise control over shell thickness and with as little as 4% standard deviation in size.²¹ The monodispersity of the sample results in a narrow distribution of exciton decay rates, making it possible to resolve changes in exciton lifetimes due to charge transfer to single molecules.

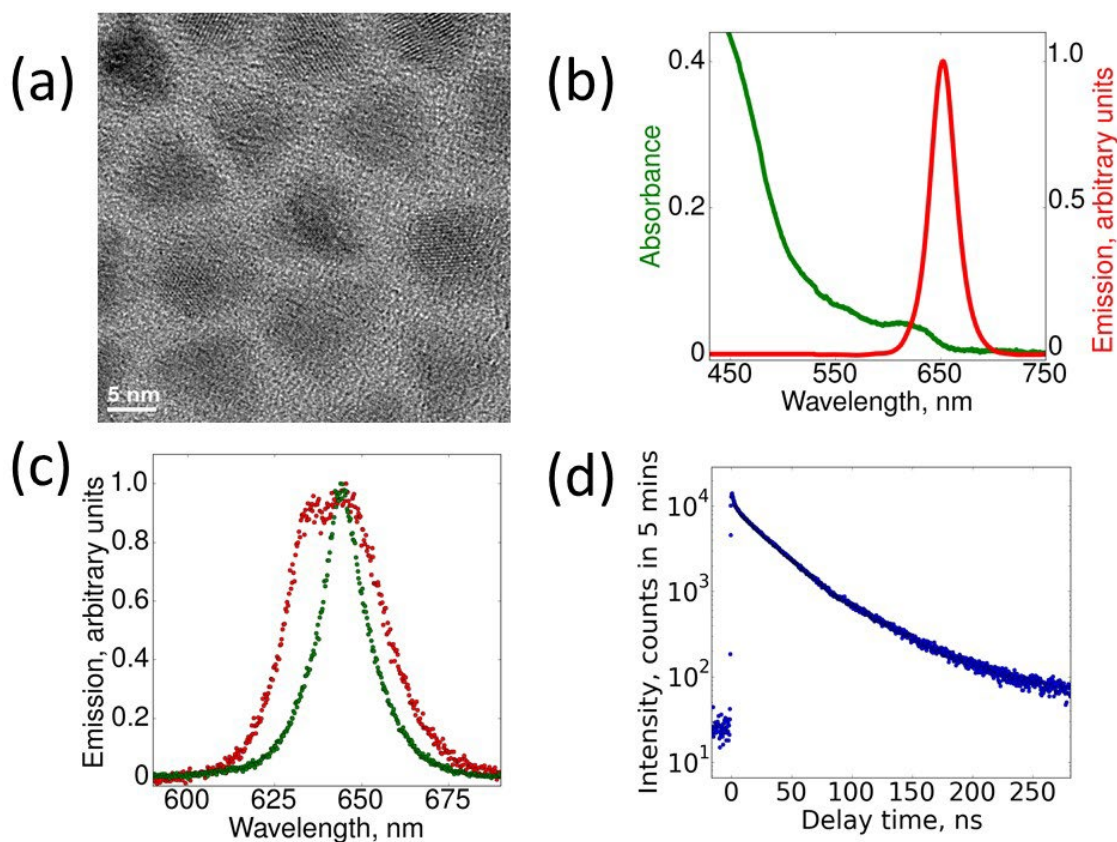


Figure 1. (a) Transmission-electron-microscope (TEM) image of CdS/CdS core-shell quantum dots (QDs). (b) Absorption (green) and emission (red) spectra of the QD ensemble in chloroform solution. (c) Emission spectra for a single QD (green) and a cluster of QDs (red). (d): Time-resolved photoluminescence from a single QD.

The core/shell QDs were synthesized using modifications of published procedures.^{21,22} The resulting nanoparticles have a quasi-spherical CdSe core and an approximately tetrahedral CdS shell, as shown in Figure 1a. The core radius is approximately 1.6 nm, and the shell thickness varies between 4 and 5 monolayers. (See the Supporting Information for details.) The lowest-energy absorption peak from the QDs occurs at a wavelength of 631 nm, and the emission peak is centered at 649 nm, as shown in Figure 1b. After the QDs were synthesized, we adsorbed methyl viologen molecules on their surfaces, as described in the Supporting Information. These molecules were selected because they have been well established by ensemble measurements as electron acceptors for CdSe QDs and CdS QDs.^{10,23-29} The adsorption procedure was designed so that a small number of viologen molecules are adsorbed on each QD, and so that aggregation of QDs in solution is minimized. The QD-viologen complexes were then deposited on a glass coverslip at low density, so that individual complexes can be resolved in a far-field optical microscope.

Single QDs on the coverslip surface were distinguished from small aggregates or clusters of QDs by measuring the linewidths of their luminescence spectra, as shown in Figure 1c: a single QD has a narrow linewidth of approximately 18 nm or less, whereas a cluster has a broader spectrum, due to differences in the sizes of the QDs making up the cluster. Figure 1c shows an example; the cluster also shows an asymmetric, flat-topped spectrum, due to the contribution of several individual QD spectra, that is qualitatively different from the single-QD spectrum. In addition, we assume that any points exhibiting unusually bright photoluminescence or not undergoing blinking (fluorescence intermittency) are clusters rather than individual QDs.

Once a single QD has been identified, its photoluminescence is resolved in time using time-correlated single-photon counting (TCSPC). (See the Supporting Information for details.) The

arrival time of each detected photon is recorded relative to the corresponding excitation laser pulse and relative to the start of the experiment. A histogram of the delay times between excitation and emission gives the time-averaged photoluminescence kinetics for the QD. As shown in Figure 1d, this total curve includes a tail at long delay times, with a time constant greater than 100 ns; this may be due to a “delayed emission” process, in which carriers are trapped on surface states for a certain amount of time before returning to the core of the quantum dot and recombining to emit a photon.^{30,31}

Even at times shorter than this slow decay tail, the time-averaged decay dynamics are still not described by a single exponential, either for QDs or QD-viologen complexes. At least part of this can be attributed to fluorescence intermittency, or blinking, of the QD, with corresponding fluctuations in the non-radiative emission rate.³² However, some previous studies have interpreted single-QD data as providing evidence that photoinduced charge-transfer rates also fluctuate over time.^{12,19,33,34} In order to determine whether this fluctuation is occurring in our samples, we divide each measurement into a series of time bins. For each bin, we generate a histogram similar to Figure 1d, only with many fewer photons. We then fit this histogram to a single exponential function to get the decay rate. In order to obtain reasonable time resolution over the experiment, the number of photons in each bin must be limited; however, the uncertainty in the lifetime increases as the number of photons in the bin decreases. We ensure that this lifetime uncertainty remains constant over the duration of the experiment and from one QD to another by adjusting the bin size so that each bin has 350 photons. We also calculate the average intensity in each bin by dividing 350 by the difference between the arrival times of the first and last photons in the bin.

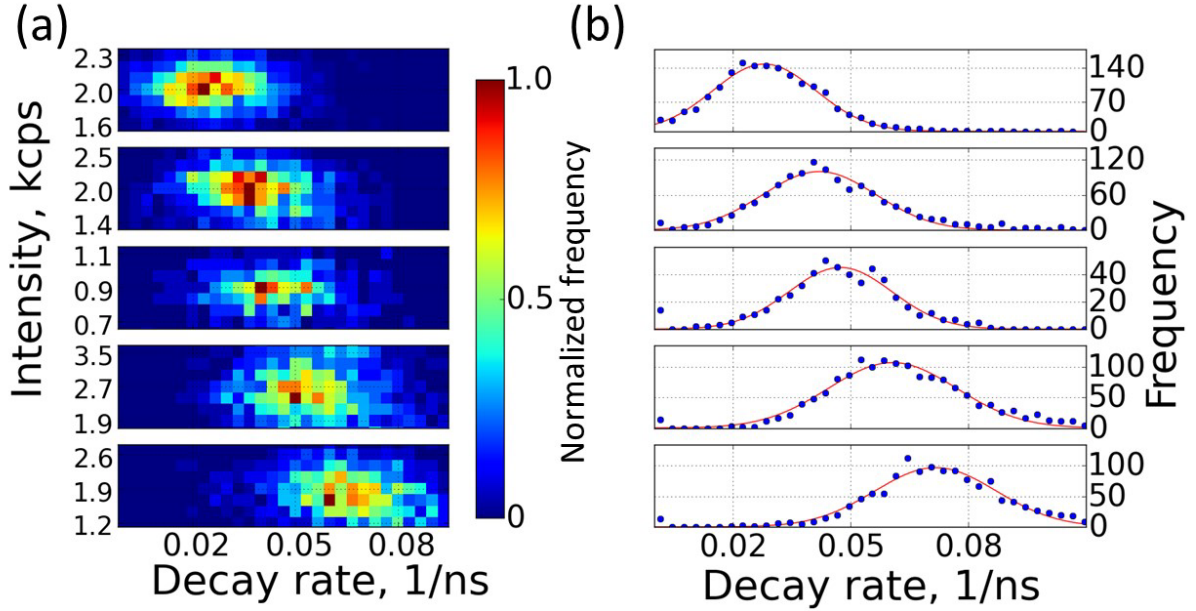


Figure 2. (a) Joint distribution of photoluminescence intensity (in thousands of counts per second, kcps) and decay rate for five individual QDs with viologen molecules adsorbed on their surfaces. The measurement is divided into time bins, each with 350 detected photons, and the average intensity and decay rate are determined for each time bin. The color scale represents the number of time bins with a given intensity and decay rate, normalized by the maximum number. (b) Distribution of decay rates, determined as in (a). Blue points are experimental data and red lines are fits to Gaussian functions. The mean decay rates for the five QDs, from top to bottom, are 0.028, 0.042, 0.047, 0.061, and 0.072 ns^{-1} , respectively. The corresponding standard deviations in the decay rates are 0.013, 0.014, 0.013, 0.016, and 0.015 ns^{-1} , respectively.

Figure 2 shows the distributions of intensities and decay rates obtained in this way for five individual QDs. Because the QDs that we study have suppressed blinking compared to conventional QDs, the distributions are dominated by the properties of the bright, emissive state of the QD. The average intensity for a particular QD depends on the efficiency with which emitted photons are collected, which in turn is sensitive to the precise alignment of the QD relative to the focus of the microscope objective and the orientation of the QD on the surface; it is thus not meaningful to compare absolute intensities from one QD to another. It is clear, however, that the relative standard deviations in the intensity and in the decay rate is constant from one QD to another, even as the average decay rate increases by a factor of approximately 2.5. These standard deviations are most likely dominated by statistical error due to the finite number of photons in each bin. We thus do not observe the dynamic heterogeneity that has been claimed in previous studies. This may be because previous studies employed different acceptor molecules, but it may also be due to the use of bins with constant time duration in the previous studies: for QDs with adsorbed acceptor molecules, the average photon detection rate is lower than it is for QDs without adsorbed molecules, so the fitting error increases when constant-duration bins are used. The apparent broadening of the lifetime distribution for QDs undergoing charge transfer in previous studies may thus simply be a statistical artifact.

For our measurements, the absence of broadening in the lifetime distribution means that we can assign to each QD a single average decay rate, which corresponds to the sum of the rate at which excitons in the QD recombine and the charge-transfer rate for that QD. In order to quantitatively account for the recombination rate, we must take into account the fluctuating non-radiative recombination rate associated with blinking. Before doing so, we examine the blinking

itself in order to determine whether its statistical properties are affected by the charge-transfer process.

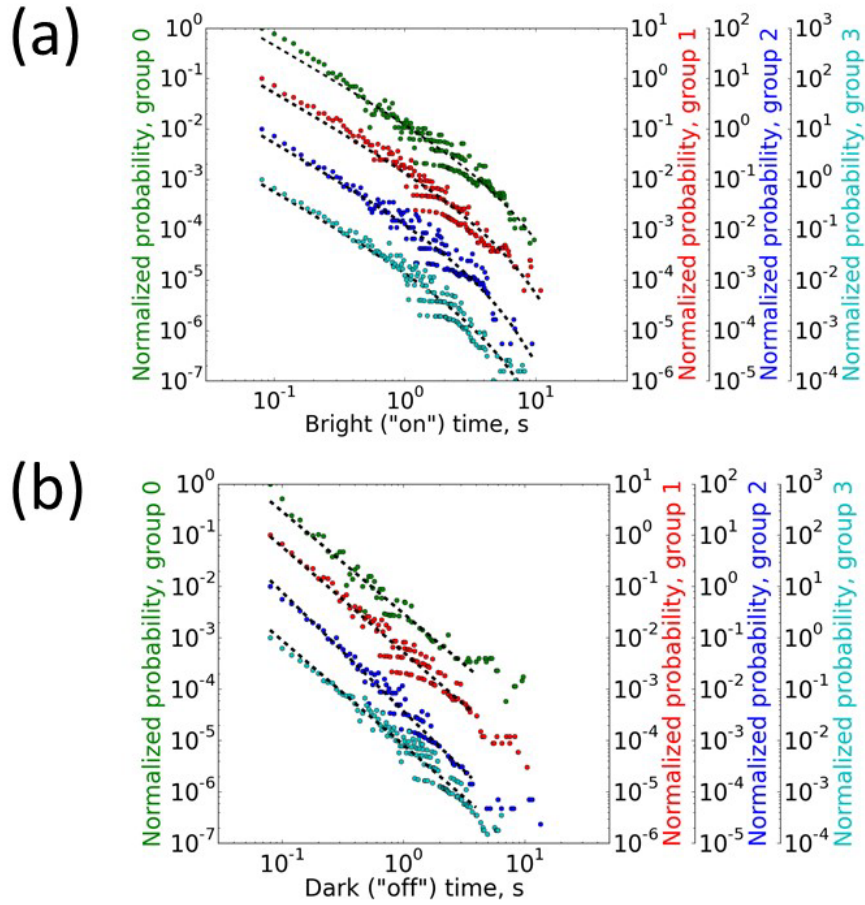


Figure 3. (a) Blinking time distributions for the bright state obtained by combining the data from several individual QDs. The QDs are sorted into three groups according to their average decay rates: groups 0 to 3 correspond to approximate decay rates of 0.03, 0.04, 0.05 and 0.06 ns^{-1} , respectively. The number for each group corresponds to the expected number of molecules adsorbed onto each QD. The distributions all follow truncated power-law distributions with exponents, α_{on} , of -1.5 and truncation times, Γ_{on} , of 0.2, 0.2, 0.3, and 0.3 s^{-1} , respectively. (b) Blinking time distributions for the dark state obtained by combining the data from several

individual QDs. The distributions all follow power-law distributions; the corresponding exponents, α_{off} , are -2.1, -2.1, -2.3, and -2.0, respectively.

Blinking statistics are most commonly described in terms of the distributions of times spent in the bright and dark states; results are shown for our samples in Figure 3.³⁵ (See the Supporting Information for details on how these distributions are calculated.) In this figure, the QDs are grouped according to their mean decay rates, and the statistics from all the QDs in each group are combined. The distributions for the dark states follow a power law, $\rho(t) = t^{-\alpha_{off/on}}$, with $\alpha_{off} = -2.1 \pm 0.1$ for all of the groups, consistent with values previously reported for similar CdSe/CdS core/shell QDs.²¹ The distribution for the bright states is fitted with a truncated power law distribution:^{36,37}

$$P(t) = A * t^{-\alpha_{on}} \exp(-\Gamma_{on} t).$$

Both the truncation time, Γ_{on} , and the power-law exponent, α_{on} , are found to be constant across the four groups, even though group 0 is not undergoing electron transfer, and groups 1 – 3 are all undergoing electron transfer at different rates. The increasing electron-transfer rate presumably reflects increasing numbers of molecules adsorbed on the QD surfaces; as demonstrated below, the number used to label each group corresponds to the number of molecules adsorbed onto the surface of each QD in the group.

Our results thus indicate that the electron-transfer process does not affect the blinking statistics. This result again contrasts previous reports of modified blinking statistics in the presence of photoinduced charge transfer.^{11,14,15} Similar to our observation of the absence of dynamic heterogeneity in photoinduced electron-transfer rates, our observation of unmodified

blinking statistics may be due to the particular QD-molecule system studied, or it may reflect statistical artifacts in previous analyses.

Taking the results for QD blinking together with the results for the single-QD lifetime distributions, we conclude that the only effect of viologen molecules on the QD surfaces is to increase the decay rate by a certain amount, with that amount being fixed for each individual QD observed. The total decay rate includes radiative decay, electron transfer, and a fluctuating non-radiative decay³². The contribution of non-radiative decay, however, can be eliminated by analyzing only photons collected when the QD is in its bright state.^{38,39} The histogram of decay times for only these photons is a single exponential for delay times between 3.5 ns and 30 ns for all of the QDs studied; an example is shown in the Supporting Information (Figure S2). There is a fast decay at delay times less than ~ 3.5 ns, most likely due to scattered laser light and charge trapping in the QD. At delay times longer than about 30 ns, the signal is dominated by shot noise. The CdS shell thickness for the core / shell QDs we use is such that the electron transfer process is expected to occur between these two limiting time scales.¹¹ We can thus determine the decay time by fitting the histogram to a single exponential for delay times between 3.5 ns and 30 ns.

Figure 4 shows distributions of decay rates determined in this way for a series of individual QDs from three separately prepared samples. Figure 4(a1) shows results for a number of QDs from a sample that was not treated with viologen molecules. These QDs show an average decay rate of 0.029 ns^{-1} , with a standard deviation of approximately 0.003 ns^{-1} . Figures 4 (b1) and (c1) show results for a number of QDs from two different, separately prepared samples of QDs with viologen molecules adsorbed randomly on their surfaces. For both collections of QDs, there is a peak with the same average decay rate as the viologen-free dots, and there are a series of evenly-

spaced peaks with higher decay rates. We can thus attribute each peak to a discrete number of viologens on each QD; *i.e.*, the lowest-rate peak corresponds to no adsorbed molecules, the next peak to one adsorbed molecule, the next peak to two adsorbed molecules, and so on. The even spacing of the peaks indicates that electron transfer to each viologen molecule is independent from electron transfer to the others, so that the total electron-transfer rate is simply the sum of the individual electron-transfer rates.¹⁰ In other words, the decay rate for each QD is given by

$$\gamma = n \times \gamma_{CT,int} + \gamma_0 \quad (1)$$

where γ_0 is the decay rate of an exciton in a QD without any viologen molecules attached; $\gamma_{CT,int}$ is the photoinduced electron transfer rate from the QD to a single viologen molecule (the intrinsic charge-transfer rate); and n is the number of viologen molecules absorbed on a given QD. This is consistent with previous ensemble measurements, where the electron transfer rate was observed to be linear in the number of adsorbed electron acceptors.¹⁰

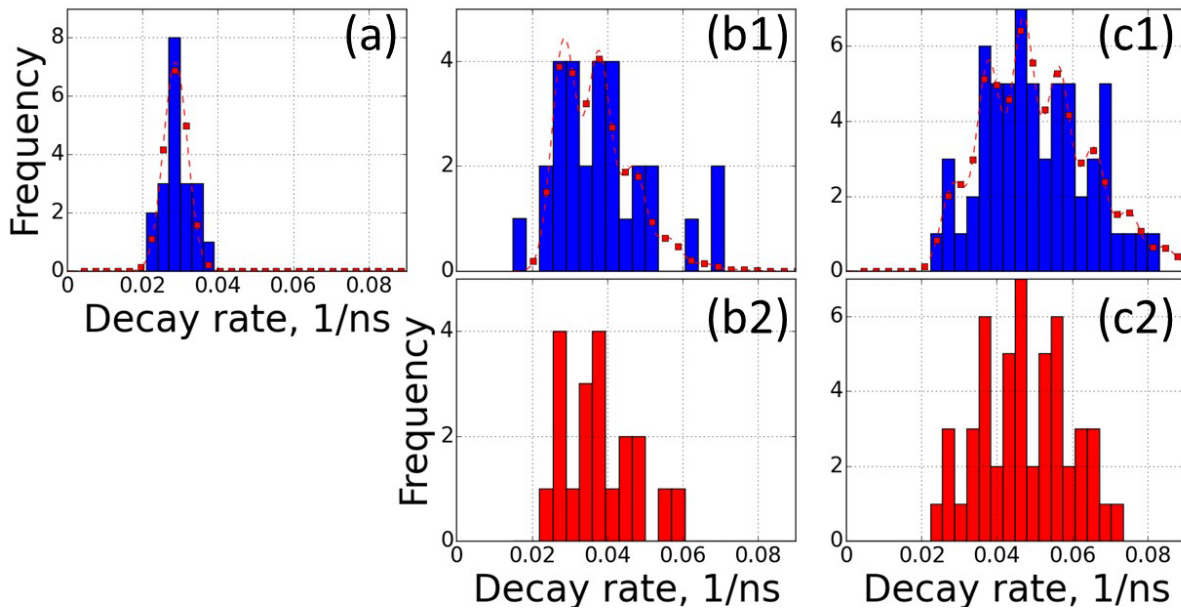


Figure 4. (a) Distribution of decay rates for 20 individual QDs with no adsorbed viologen molecules. The results correspond to the distribution of radiative recombination rates in the quantum-dot sample. The bars are experimental data, and the points are a Gaussian fit with a center at 0.029 ns^{-1} and a width of 0.003 ns^{-1} . (b1, c1) Distribution of decay rates for 29 and 62 QDs, respectively, with adsorbed viologen molecules, from two different, separately prepared samples. The separate peaks correspond to different discrete numbers of viologen molecules on the QD surfaces. The points are simulated distributions using the Gaussian fit from (a), a constant electron-transfer rate of 0.009 ns^{-1} per molecule, and a Poisson distribution of molecules on the QD surfaces. (b2, c2) Simulated distributions using the raw experimental data from (a), a constant electron-transfer rate of 0.009 ns^{-1} per molecule, and a Poisson distribution of molecules on the QD surfaces. Simulated frequency values are rounded to the nearest integer.

If each viologen molecule adsorbs independently onto a given QD, then the number of molecules adsorbed on each QD will follow a binomial distribution.⁹ If the average number of viologens bound to each QD is much less than the number of available binding sites, then the binomial distribution is well approximated by a Poisson distribution.^{40,41} The distribution of decay rates is then described by

$$P(\gamma) = \sum_{n=0}^{\infty} \frac{\lambda^n e^{-\lambda}}{n!} \times p_0(\gamma_0 + n \times \gamma_{CT,int}), \quad (2)$$

where $p_0(\gamma_0)$ is the decay-rate distribution for QDs with no viologen molecules and λ is the average number of molecules adsorbed per quantum dot. In order to compare this model to experiment, we can take $p_0(\gamma_0)$ in one of two ways: (1) from a Gaussian fit to the experimentally measured decay-rate distribution for the control group that has not been treated with viologen, or (2) directly from the experimental distribution for this control group. Figures 4 (b1) and (c1)

show the modeled distribution obtained using the first method, and Figures 4 (b2) and (c2) show the modeled distribution obtained using the second method. Good agreement between expected and measured distributions are obtained for the two collections of QD-viologen complexes by using the same value, $\gamma_A = 0.009 \text{ ns}^{-1}$, for the electron-transfer rate from a single QD to a single adsorbed viologen molecule. The only remaining fitting parameter is λ , the average number of viologens per QD; unlike γ_A , this parameter is different for the two collections of QD-viologen complexes. Most differences between the simulated and measured distributions are attributable to statistical variations due to the finite number of QDs measured for each sample.

The measured electron-transfer rate of 0.009 ns^{-1} from a QD to a single adsorbed viologen molecule is similar to the electron-transfer rate inferred from previous single-dot studies from core/shell QDs with comparable shell thicknesses to adsorbed fluorescein molecules.¹¹ The results are thus consistent with the assumption that the total electron-transfer rate for a QD with n molecules on its surface is simply n times the electron-transfer rate to a single molecule; that is, electron transfer to each viologen molecule on the surface of a given QD is independent from electron transfer to the other molecules on the surface of the same QD. Moreover, the electron-transfer rate appears to be the same for all viologen molecules adsorbed on QD surfaces, despite the fact that the shell thickness varies across the surface of each QD. This most likely implies that the difference in electron-transfer rate for molecules adsorbed at different locations is smaller than the natural variation in decay rates among the QDs in the ensemble, so that the variation in electron-transfer rate does not significantly broaden the peaks in the distribution of decay times. In addition, the distribution may be dominated by electron transfer to viologen molecules that are located closest to the QD cores and thus have the fastest transfer rate. This possibility is supported by the fact that the agreement between theory and measurement appears

to be somewhat poorer for faster decay rates, suggesting there are more dots observed with fast decay rates than would be expected on the basis of a single intrinsic electron-transfer rate and Poisson statistics for the number of adsorbed molecules.

Determining whether there is any discrepancy between the simple model of Eq. (2) and experiment will require measuring a larger number of QDs from each sample. Currently, this number is limited by the stability the sample: measurements were made over at most two days on a single sample because the viologen molecules appeared to degrade⁴² or desorb from the QD surfaces over longer time scales. In order to measure more individual QDs and obtain greater statistical significance, an improvement in sample stability will be required.

As a validation of our single-QD results, we perform time-resolved photoluminescence measurements for the ensemble of QDs in solution. The results are shown in Figure 5, and are fit by assuming a Poisson distribution of viologen molecules on the QDs:¹⁰

$$I(t) = \sum_{n=0}^{\infty} \frac{\lambda^n e^{-\lambda}}{n!} \times I_0(t) \times e^{-n \times \gamma_{CT,int} t} \quad (3)$$

where $I_0(t)$ is the decay curve of quantum dots in solution with no viologen molecules (measured experimentally, as shown in Figure 5). A fit using the electron-transfer rate $\gamma_{CT,int} = 0.009 \text{ ns}^{-1}$ from the single-dot measurements is in good agreement with the ensemble measurements for delay times from approximately 7 ns to 30 ns; the only free parameter in this fit is λ . For shorter decay times, there is a fast decay that is not fit by the model. This can be attributed to small clusters of QDs in solution,⁴³ which are known to have fast decays due to energy transfer among the QDs in the clusters. Because the clusters emit more intensely than individual QDs, even a small fraction of clusters can affect the observed ensemble dynamics. In our single-QD measurements, we can exclude these clusters from the analysis based on their

photoluminescence linewidths, intensities, and blinking characteristics; this selectivity is one advantage of the single-particle approach.

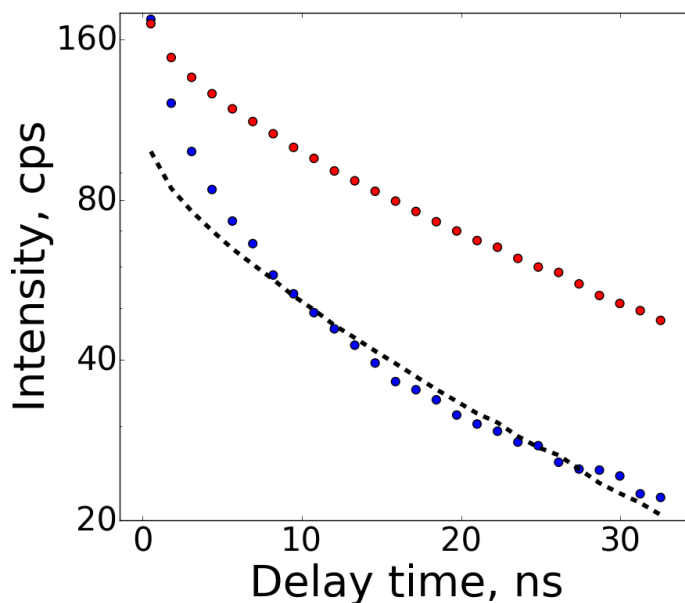


Figure 5. Time-resolved photoluminescence for QDs in chloroform solution, in counts per second (cps). Red circles are for QDs alone and blue circles are for QDs with adsorbed viologen molecules. The black dashed line is a fit to the QDs with viologen, using a single-molecule photoinduced electron-transfer rate of 0.009 ns^{-1} and an average of 1.0 adsorbed viologens per QD.

In summary, we measured the photoinduced electron transfer rate from individual CdSe/CdS core/shell quantum dots to methyl viologen molecules adsorbed on their surfaces. Each dot exhibits a constant single donor-acceptor transfer rate ($0.009 \pm 0.003 \text{ ns}^{-1}$). Since this rate exceeds the standard deviation in the excited-state decay rates among the QDs in the sample, we are able

for the first time to resolve the number of acceptor molecules adsorbed on a given QD using the total photoluminescence decay rate of the QD. In other words, we are able to count, through optical measurements, the number of acceptor molecules adsorbed on the surface of a particular QD. This opens up new possibilities for the detection of individual molecules that do not fluoresce and whose optical absorption and scattering cross-sections are too small to allow for direct measurement, with potential applications in biosensing.⁴⁴ It may also be possible to monitor the adsorption and desorption of individual acceptor molecules from QD surfaces through real-time changes in charge-transfer rates. Using anisotropic nanocrystals, such as core-shell nanorods⁴⁵ and nanoplatelets,⁴⁶ will enable studies of how photoinduced electron transfer depends on the spatial location of the acceptor molecule on the nanoparticle surface. Selective excitation of particular transitions in the nanocrystals will enable studies of how photoinduced electron-transfer dynamics interact with charge relaxation and localization dynamics within the nanocrystals.⁴⁷ In order to enable these future measurements, it will be necessary to improve the long-term stability of the nanocrystal-acceptor complexes, so that a statistically significant number of complexes can be characterized before the properties of the sample change. It will also be advantageous to synthesize ensembles of nanocrystals with very narrow distributions of radiative decay times, so that changes in dynamics due to electron transfer can easily be distinguished from heterogeneity in the sample. With these improvements, single-QD / single-molecule charge-transfer measurements should provide the mechanistic understanding required to engineer charge-transfer dynamics at the nanoscale, enabling the optimization of applications including photocatalysis and low-cost photovoltaics.

ACKNOWLEDGMENT

This project was supported by the Institute for Sustainability and Energy at Northwestern and by the National Institute of Standards and Technology under award number 14D295. This material is based upon work supported by the National Science Foundation through a Graduate Research Fellowship to V.A.A. (Grant No. DGE-1324585). Electron microscopy was performed in the NUANCE Center at Northwestern University. NUANCE is supported by the International Institute for Nanotechnology, MRSEC (NSF DMR-1121262), the Keck Foundation, the State of Illinois, and Northwestern University. This work was performed, in part, at the Center for Nanoscale Materials, a U.S. Department of Energy Office of Science User Facility under Contract No. DE-AC02-06CH11357. The authors would like to thank Dmitriy Dolzhenkov for his help in acquiring electron microscope images of the particles.

SUPPORTING INFORMATION

Details on synthesis of CdSe/CdS core/shell QDs, preparation of QD / methyl-viologen complexes, optical measurements, and characterization of QD blinking.

REFERENCES

- (1) Halim, M. A. Harnessing Sun's Energy with Quantum Dots Based Next Generation Solar Cell. *Nanomaterials* **2013**, *3*, 22-47.
- (2) Hillhouse, H. W.; Beard, M. C. Solar Cells from Colloidal Nanocrystals: Fundamentals, Materials, Devices, and Economics. *Curr. Opin. in Colloid Interface Sci.* **2009**, *14*, 245-259.
- (3) Kamat, P. V. Manipulation of Charge Transfer Across Semiconductor Interface. A Criterion That Cannot Be Ignored in Photocatalyst Design. *J. Phys. Chem. Lett.* **2012**, *3*, 663-672.
- (4) Adams, D. M.; Brus, L.; Chidsey, C. E. D.; Creager, S.; Creutz, C.; Kagan, C. R.; Kamat, P. V.; Lieberman, M.; Lindsay, S.; Marcus, R. A.; *et al.* Charge Transfer on the Nanoscale: Current Status. *J. Phys. Chem. B* **2003**, *107*, 6668-6697.

- (5) Knowles, K. E.; Peterson, M. D.; McPhail, M. R.; Weiss, E. A. Exciton Dissociation within Quantum Dot-Organic Complexes: Mechanisms, Use as a Probe of Interfacial Structure, and Applications. *J. Phys. Chem. C* **2013**, *117*, 10229-10243.
- (6) Robel, I.; Kuno, M.; Kamat, P. V. Size-Dependent Electron Injection from Excited CdSe Quantum Dots into TiO₂ Nanoparticles. *J. Am. Chem. Soc.* **2007**, *129*, 4136-4137.
- (7) Dibbell, R. S.; Watson, D. F. Distance-Dependent Electron Transfer in Tethered Assemblies of CdS Quantum Dots and TiO₂ Nanoparticles. *J. Phys. Chem. C* **2009**, *113*, 3139-3149.
- (8) Tvrđy, K.; Frantsuzov, P. A.; Kamat, P. V. Photoinduced Electron Transfer from Semiconductor Quantum Dots to Metal Oxide Nanoparticles. *Proc. Natl. Acad. Sci. USA* **2011**, *108*, 29-34.
- (9) Sadhu, S.; Tachiya, M.; Patra, A. A. Stochastic Model for Energy Transfer from CdS Quantum Dots/Rods (Donors) to Nile Red Dye (Acceptors). *J. Phys. Chem. C* **2009**, *113*, 19488-19492.
- (10) Morris-Cohen, A. J.; Frederick, M. T.; Cass, L. C.; Weiss, E. A. Simultaneous Determination of the Adsorption Constant and the Photoinduced Electron Transfer Rate for a CdS Quantum Dot-Viologen Complex. *J. Am. Chem. Soc.* **2011**, *133*, 10146-10154.
- (11) Jin, S.; Hsiang, J.-C.; Zhu, H.; Song, N.; Dickson, R. M.; Lian, T. Correlated Single Quantum Dot Blinking and Interfacial Electron Transfer Dynamics. *Chem. Sci.* **2010**, *1*, 519-526.
- (12) Song, N.; Zhu, H.; Jin, S.; Lian, T. Hole Transfer from Single Quantum Dots. *ACS Nano* **2011**, *5*, 8750-8759.
- (13) Liu, Z.; Zhu, H.; Song, N.; Lian, T. Probing Spatially Dependent Photoinduced Charge Transfer Dynamics to TiO₂ Nanoparticles Using Single Quantum Dot Modified Atomic Force Microscopy Tips. *Nano Lett.* **2013**, *13*, 5563-5569.
- (14) Zang, H.; Routh, P. K.; Alam, R.; Maye, M. M.; Cotlet, M. Core Size Dependent Hole Transfer from a Photoexcited CdSe/ZnS Quantum Dot to a Conductive Polymer. *Chem. Commun.* **2014**, *50*, 5958-5960.
- (15) Xu, Z.; Cotlet, M. Photoluminescence Blinking Dynamics of Colloidal Quantum Dots in the Presence of Controlled External Electron Traps. *Small* **2012**, *8*, 253-258.
- (16) Hadar, I.; Halivni, S.; Even-Dar, N. A.; Faust, A.; Banin, U. Dimensionality Effects on Fluorescence Resonance Energy Transfer between Single Semiconductor Nanocrystals and Multiple Dye Acceptors. *J. Phys. Chem. C* **2015**, *119*, 3849-3856.
- (17) Xu, B. Q.; Tao, N. J. J. Measurement of Single-Molecule Resistance by Repeated Formation of Molecular Junctions. *Science* **2003**, *301*, 1221-1223.
- (18) Zhu, H.; Song, N.; Lian, T. Controlling Charge Separation and Recombination Rates in CdSe/ZnS Type I Core-Shell Quantum Dots by Shell Thicknesses. *J. Am. Chem. Soc.* **2010**, *132*, 15038-15045.
- (19) Xu, Z.; Hine, C. R.; Maye, M. M.; Meng, Q.; Cotlet, M. Shell Thickness Dependent Photoinduced Hole Transfer in Hybrid Conjugated Polymer/Quantum Dot Nanocomposites: From Ensemble to Single Hybrid Level. *ACS Nano* **2012**, *6*, 4984-4992.
- (20) Zhu, H.; Song, N.; Lian, T. Wave Function Engineering for Ultrafast Charge Separation and Slow Charge Recombination in Type II Core/Shell Quantum Dots. *J. Am. Chem. Soc.* **2011**, *133*, 8762-8771.

- (21) Chen, O.; Zhao, J.; Chauhan, V. P.; Cui, J.; Wong, C.; Harris, D. K.; Wei, H.; Han, H.-S.; Fukumura, D.; Jain, R. K.; *et al.* Compact High-Quality CdSe-CdS Core-Shell Nanocrystals with Narrow Emission Linewidths and Suppressed Blinking. *Nat. Mater.* **2013**, *12*, 445-451.
- (22) Carbone, L.; Nobile, C.; De Giorgi, M.; Sala, F. D.; Morello, G.; Pompa, P.; Hytch, M.; Snoeck, E.; Fiore, A.; Franchini, I. R.; *et al.* Synthesis and Micrometer-Scale Assembly of Colloidal CdSe/CdS Nanorods Prepared by a Seeded Growth Approach. *Nano Lett.* **2007**, *7*, 2942-2950.
- (23) Yang, Y.; Lian, T. Multiple Exciton Dissociation and Hot Electron Extraction by Ultrafast Interfacial Electron Transfer from PbS QDs. *Coord. Chem. Rev.* **2014**, *263*, 229-238.
- (24) Peterson, M. D.; Jensen, S. C.; Weinberg, D. J.; Weiss, E. A. Mechanisms for Adsorption of Methyl Viologen on CdS Quantum Dots. *Acs Nano* **2014**, *8*, 2826-2837.
- (25) Zhu, H.; Song, N.; Rodriguez-Cordoba, W.; Lian, T. Wave Function Engineering for Efficient Extraction of up to Nineteen Electrons from One CdSe/CdS Quasi-Type II Quantum Dot. *J. Am. Chem. Soc.* **2012**, *134*, 4250-4257.
- (26) Dworak, L.; Matylitsky, V. V.; Breus, V. V.; Braun, M.; Basche, T.; Wachtveitl, J. Ultrafast Charge Separation at the CdSe/CdS Core/Shell Quantum Dot/Methylviologen Interface: Implications for Nanocrystal Solar Cells. *J. Phys. Chem. C* **2011**, *115*, 3949-3955.
- (27) Matylitsky, V. V.; Dworak, L.; Breus, V. V.; Basche, T.; Wachtveitl, J. Ultrafast Charge Separation in Multiexcited CdSe Quantum Dots Mediated by Adsorbed Electron Acceptors. *J. Am. Chem. Soc.* **2009**, *131*, 2424-2425.
- (28) Logunov, S.; Green, T.; Marguet, S.; El-Sayed, M. A. Interfacial Carriers Dynamics of CdS Nanoparticles. *J. Phys. Chem. A* **1998**, *102*, 5652-5658.
- (29) Wang, Y.-F.; Wang, H.-Y.; Li, Z.-S.; Zhao, J.; Wang, L.; Chen, Q.-D.; Wang, W.-Q.; Sun, H.-B. Electron Extraction Dynamics in CdSe and CdSe/CdS/ZnS Quantum Dots Adsorbed with Methyl Viologen. *J. Phys. Chem. C* **2014**, *118*, 17240-17246.
- (30) Jones, M.; Lo, S. S.; Scholes, G. D. Quantitative Modeling of the Role of Surface Traps in CdSe/CdS/ZnS Nanocrystal Photoluminescence Decay Dynamics. *Proc. Natl. Acad. Sci. USA* **2009**, *106*, 3011-3016.
- (31) Rabouw, F. T.; Kamp, M.; van Dijk-Moes, R. J. A.; Gamelin, D. R.; Koenderink, A. F.; Meijerink, A.; Vanmaekelbergh, D. Delayed Exciton Emission and Its Relation to Blinking in CdSe Quantum Dots. *Nano Lett.* **2015**, *15*, 7718-7725.
- (32) Fisher, B. R.; Eisler, H. J.; Stott, N. E.; Bawendi, M. G. Emission Intensity Dependence and Single-Exponential Behavior in Single Colloidal Quantum Dot Fluorescence Lifetimes. *J. Phys. Chem. B* **2004**, *108*, 143-148.
- (33) Issac, A.; Jin, S.; Lian, T. Intermittent Electron Transfer Activity From Single CdSe/ZnS Quantum Dots. *J. Am. Chem. Soc.* **2008**, *130*, 11280-11281.
- (34) Song, N.; Zhu, H.; Liu, Z.; Huang, Z.; Wu, D.; Lian, T. Unraveling the Exciton Quenching Mechanism of Quantum Dots on Antimony-Doped SnO₂ Films by Transient Absorption and Single Dot Fluorescence Spectroscopy. *ACS Nano* **2013**, *7*, 1599-1608.
- (35) Kuno, M.; Fromm, D. P.; Hamann, H. F.; Gallagher, A.; Nesbitt, D. J. Nonexponential "Blinking" Kinetics of Single CdSe Quantum Dots: A Universal Power Law Behavior. *J. Chem. Phys.* **2000**, *112*, 3117-3120.

- (36) Tang, J.; Marcus, R. A. Mechanisms of Fluorescence Blinking in Semiconductor Nanocrystal Quantum Dots. *J. Chem. Phys.* **2005**, *123*, 054704.
- (37) Cui, S.-C.; Tachikawa, T.; Fujitsuka, M.; Majima, T. Interfacial Electron Transfer Dynamics in a Single CdTe Quantum Dot-Pyromellitimide Conjugate. *J. Phys. Chem. C* **2008**, *112*, 19625-19634.
- (38) Galland, C.; Ghosh, Y.; Steinbrueck, A.; Sykora, M.; Hollingsworth, J. A.; Klimov, V. I.; Htoon, H. Two Types of Luminescence Blinking Revealed by Spectroelectrochemistry of Single Quantum Dots. *Nature* **2011**, *479*, 203-207.
- (39) Wu, X.; Sun, Y.; Pelton, M. Recombination Rates for Single Colloidal Quantum Dots Near a Smooth Metal Film. *Phys. Chem. Chem. Phys.* **2009**, *11*, 5867-5870.
- (40) Morris-Cohen, A. J.; Vasilenko, V.; Amin, V. A.; Reuter, M. G.; Weiss, E. A. Model for Adsorption of Ligands to Colloidal Quantum Dots with Concentration-Dependent Surface Structure. *ACS Nano* **2012**, *6*, 557-565.
- (41) M. Tachiya; Kinetics of Quenching of Luminescent Probes in Micellar Systems. II. *J. Chem. Phys.* **1982**, *76*, 340-348.
- (42) Tagliazucchi, M.; Amin, V. A.; Schneebeli, S. T.; Stoddart, J. F.; Weiss, E. A. High-Contrast Photopatterning of Photoluminescence within Quantum Dot Films through Degradation of a Charge-Transfer Quencher. *Adv. Mater.* **2012**, *24*, 3617-3621.
- (43) Morris-Cohen, A. J.; Donakowski, M. D.; Knowles, K. E.; Weiss, E. A. The Effect of a Common Purification Procedure on the Chemical Composition of the Surfaces of CdSe Quantum Dots Synthesized with Trioctylphosphine Oxide. *J. Phys. Chem. C* **2010**, *114*, 897-906.
- (44) Cordes, D. B.; Gamsey, S.; Sharrett, Z.; Miller, A.; Thoniyot, P.; Wessling, R. A.; Singaram, B. The Interaction of Boronic Acid-Substituted Viologens with Pyranine: The Effects of Quencher Charge on Fluorescence Quenching and Glucose Response. *Langmuir* **2005**, *21*, 6540-6547.
- (45) Talapin, D. V.; Koepe, R.; Gotzinger, S.; Kornowski, A.; Lupton, J. M.; Rogach, A. L.; Benson, O.; Feldmann, J.; Weller, H. Highly Emissive Colloidal CdSe/CdS Heterostructures of Mixed Dimensionality. *Nano Lett.* **2003**, *3*, 1677-1681.
- (46) Ithurria, S.; Tessier, M. D.; Mahler, B.; Lobo, R. P. S. M.; Dubertret, B.; Efros, A. L. Colloidal Nanoplatelets with Two-Dimensional Electronic Structure. *Nat. Mater.* **2011**, *10*, 936-941.
- (47) Tisdale, W. A.; Williams, K. J.; Timp, B. A.; Norris, D. J.; Aydil, E. S.; Zhu, X. Y. Hot-Electron Transfer from Semiconductor Nanocrystals. *Science* **2010**, *328*, 1543-1547.